

Proteome-wide prediction of mode of inheritance and molecular mechanism underlying genetic diseases using structural interactomics

Ali Saadat^{1,2} and Jacques Fellay^{1,2,3,*}

¹School of Life Sciences, Ecole Polytechnique Fédérale de Lausanne, Lausanne, Switzerland

²Swiss Institute of Bioinformatics, Lausanne, Switzerland

³Precision Medicine Unit, Biomedical Data Science Center, Lausanne University Hospital and University of Lausanne, Lausanne, Switzerland

*Correspondence: jacques.fellay@epfl.ch

SUMMARY

Genetic diseases can be classified according to their modes of inheritance and their underlying molecular mechanisms. Autosomal dominant disorders often result from DNA variants that cause loss-of-function, gain-of-function, or dominant-negative effects, while autosomal recessive diseases are primarily linked to loss-of-function variants. In this study, we introduce a graph-of-graphs approach that leverages protein-protein interaction networks and high-resolution protein structures to predict the mode of inheritance of diseases caused by variants in autosomal genes, and to classify dominant-associated proteins based on their functional effect. Our approach integrates graph neural networks, structural interactomics and topological network features to provide proteome-wide predictions, thus offering a scalable method for understanding genetic disease mechanisms.

KEYWORDS

Graph neural networks, protein structure, mode of inheritance, graph-of-graphs, protein-protein interaction, genetic diseases

INTRODUCTION

Most human genetic diseases result from variants that disrupt protein function through diverse molecular mechanisms, which play a critical role in determining their mode of inheritance (MOI)¹. In autosomal dominant (AD) disorders, a single copy of a mutated gene can result in disease, often through loss of function (LOF) due to haploinsufficiency (HI), where the remaining wild-type allele cannot compensate for the lost function². Dominant disorders can also result from non-LOF mechanisms, such as gain of function (GOF), where the mutant protein acquires a new or altered function, and the dominant-negative (DN) effect, where the mutant protein interferes with the normal function of the wild-type protein³. In contrast, autosomal recessive (AR) disorders require variants in both gene copies, predominantly involving LOF mechanisms, such as missense variants that destabilize protein structure or nonsense variants leading to truncated, non-functional proteins.

Previous studies on MOI prediction have introduced computational tools such as DOMINO⁴, which utilizes linear discriminant analysis (LDA) to predict whether a protein is associated with AD disorders by integrating various features such as genomic data, conservation, and protein interactions. MOI-Pred⁵, on the other hand, focuses on variant-level predictions, specifically targeting missense variants associated with AR diseases.

More recent research has aimed at predicting the functional impact of variants in specific genes. LoGoFunc combines gene-, protein-, and variant-level features to predict pathogenic GOF, LOF, and neutral variants⁶. Another study explored the structural effects of variants, finding that non-LOF variants tend to have milder impacts on protein structure⁷. Additionally, a recent study employed three support vector machines (SVM) to predict protein coding genes associated with DN, GOF, and HI mechanisms⁸.

In this study, we present a comprehensive approach for predicting the MOI for all proteins encoded by autosomal genes, as well as elucidating the functional effect of variants underlying AD genetic disorders (Figure 1). Our framework combines graph neural networks (GNNs)⁹ with structural interactomics by creating a graph-of-graphs¹⁰, utilizing both protein-protein interaction (PPI) network and high-resolution protein structures. For MOI prediction, we model proteins as nodes within the PPI network, incorporating topological and protein-level features for classification. For molecular mechanism prediction, we represent each protein as a graph of amino acid residues, leveraging structure-based features to classify the functional effect as HI, GOF, or DN.

This integrated approach enables proteome-wide prediction of inheritance patterns and provides mechanistic insights into AD diseases, offering a novel, scalable framework for understanding genetic disorders.

For the sake of flow and conciseness, we refer to "proteins associated with AD disorders" as AD proteins and "proteins associated with AR disorders" as AR proteins. Similarly, we use DN (GOF/LOF) proteins instead of "proteins associated with DN (GOF/LOF) molecular disease mechanisms".

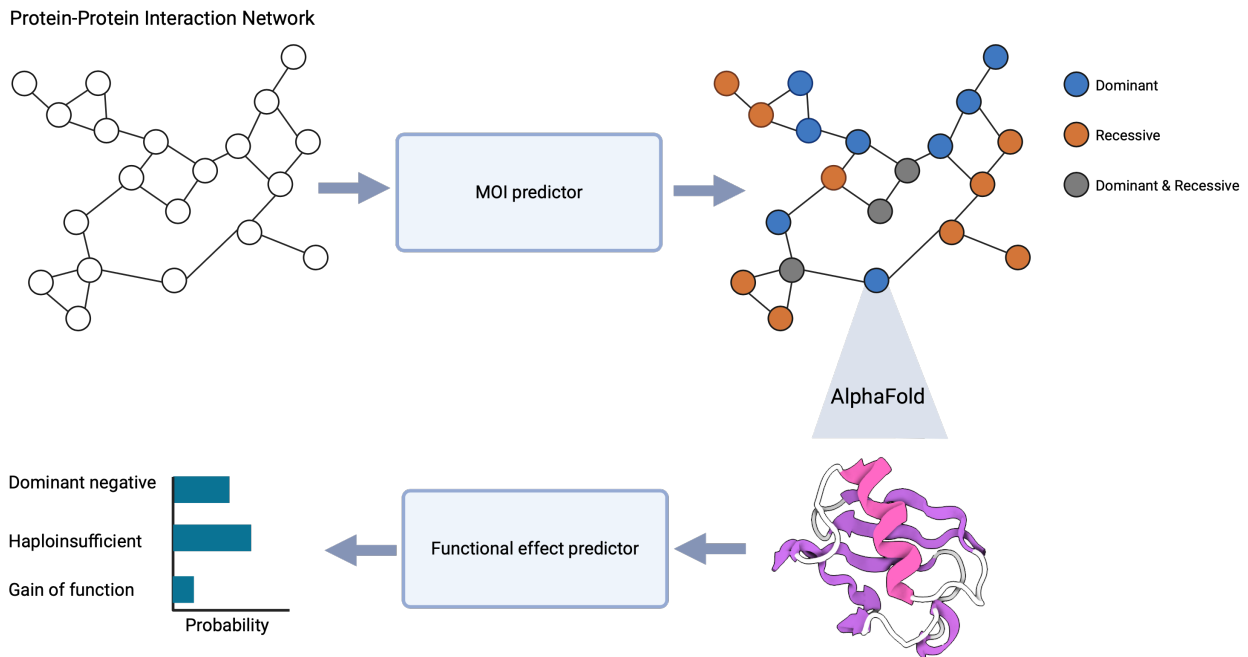


Figure 1: Overview of the study: at first the mode of inheritance (MOI) is predicted for all of the autosomal proteins in the protein-protein interaction network. Afterwards, AlphaFold protein structures are used to generate residue graphs for each dominant protein, and functional effects are predicted based on these graphs. Figure created with BioRender.com.

RESULTS

61

Datasets

62

MOI data We gathered 4,737 MOI-labeled proteins, among them 2,494 (53%) were only AR, 1,420 (30%) were only AD, and 808 (17%) were both AD and AR (Figure 2, left).

63

64

Functional effect data We collected 1,276 proteins with annotated functional effect, among them 250 (20%) were only DN, 376 (29%) were only HI, 251 (20%) were only GOF, 114 (9%) were both DN and HI, 115 (9%) were both DN and GOF, 92 (7%) were both HI and GOF, and 78 (6%) were all of the DN, HI, GOF (Figure 2, right).

65

66

67

68

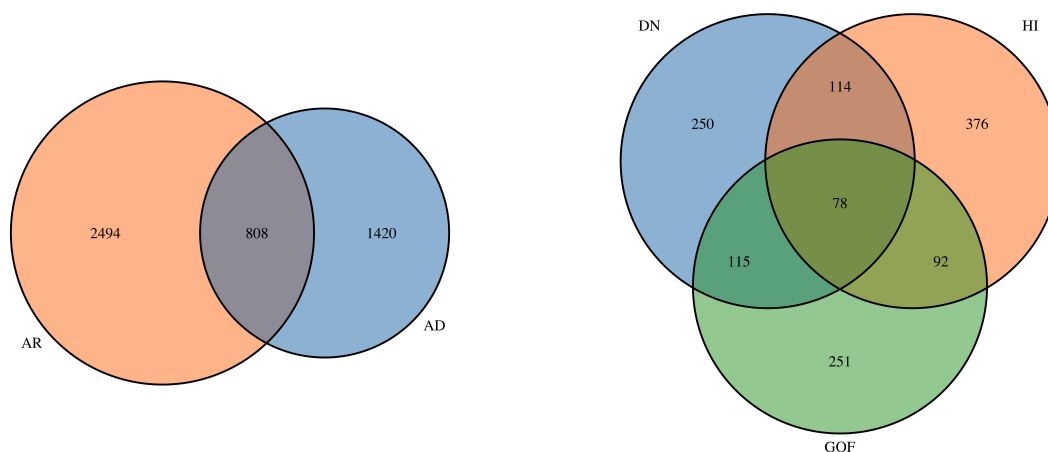


Figure 2: The number of proteins with labeled MOI (left) and molecular mechanism (right).

PPI construction and annotation We constructed a comprehensive PPI network comprising 17,248 nodes and 375,494 edges by integrating interactions from STRINGdb¹¹, BioGRID¹², the Human Reference Interactome (HuRI)¹³, and Menche et al.¹⁴. To characterize proteins, we annotated them with 78 selected features covering structural, functional, evolutionary, and regulatory properties (Supplementary Table 1).

69

70

71

72

73

Protein graph construction and annotation We obtained predicted protein structures from the AlphaFold database¹⁵ and constructed residue-level graphs using Graphein¹⁶. In these graphs, nodes represent amino acids, while edges capture peptide bonds, hydrogen bonds, disulfide bonds, ionic interactions, and other structural contacts, including long-range interactions. We annotated amino acid residues with 73 selected features reflecting structural, sequence-based, biochemical, and evolutionary characteristics (Supplementary Table 2).

74

75

76

77

78

79

Model development

80

Study design We formulated MOI prediction as a node classification task within the PPI network and functional effect prediction as a graph classification task. Both models employed a multi-label classification approach, allowing each input to have multiple labels. We evaluated various graph neural network architectures, including graph convolutional networks (GCN)¹⁷, graph attention networks (GAT)¹⁸, and graph isomorphism networks (GIN)¹⁹.

81

82

83

84

85

Data splitting To create training, validation, and test sets, we clustered protein sequences using MMseqs2²⁰ with thresholds of 20% coverage and 20% sequence identity. Proteins were then split into 80% training, 10% validation, and 10% test sets.

Hyperparameter tuning and model training All models used a single hidden layer, with the output layer containing two units for MOI prediction (AD and AR) and three units for functional effect prediction (DN, HI, and GOF). To determine the optimal configurations, we evaluated 25 hyperparameter combinations on the validation set, varying the hidden layer size across five values (128, 64, 32, 16, and 8) and the learning rate across five values ranging from 10^{-2} to 5×10^{-4} . The results of hyperparameter tuning for MOI and functional effect prediction are provided in Supplementary Tables 3 and 4. Using the selected hyperparameters, we trained each model with binary cross-entropy loss for up to 100 epochs, applying early stopping based on validation loss to prevent overfitting.

Models performance evaluation

MOI models We evaluated all trained models on the unseen test set (Table 1). The GCN model achieved the highest precision score, while the GAT model had the best recall and F_1 score. Due to the class imbalance in the MOI dataset, we prioritized maximizing F_1 score and selected the GAT model. We also assessed the performance of DOMINO⁴ as outlined in the methods section, and found that our models outperformed it (Table 1).

Functional effect models Table 2 shows the performance of various models on the functional effect test set, with the GCN model achieving the highest F_1 score. We also evaluated the SVM models from Badonyi and Marsh⁸ as described in the methods section. Based on the overall performance, we selected the GCN model for functional effect prediction.

Models interpretation

MOI feature attribution Using the GAT model, we calculated features attribution separately for correctly predicted AD or AR proteins in the test set. We observed that the most important predictors for AD prediction are features related to constraint and conservation (Figure 3 left). The top feature was UNEECON, which measures the evolutionary pressure²¹. Using the labeled data, we observed that AD proteins have higher UNEECON values compared to AR proteins (Figure 3 right).

For AR prediction, the most important feature was pLI, which is probability of loss-of-function intolerance²² (Figure 4 left). Using the ground truth dataset, we observed that AR proteins have lower pLI values compared to AD proteins (Figure 4 right).

Table 1: MOI prediction performance on the test set

| Metric | GCN | GAT | GIN | LDA ⁴ |
|-----------|--------------|--------------|-------|------------------|
| F1 | 0.745 | 0.750 | 0.671 | 0.685 |
| Precision | 0.776 | 0.770 | 0.764 | 0.721 |
| Recall | 0.725 | 0.731 | 0.621 | 0.654 |

Table 2: Functional effect prediction performance on the test set

| Metric | GCN | GAT | GIN | SVM ⁸ |
|-----------|--------------|--------------|-------|------------------|
| F1 | 0.627 | 0.590 | 0.600 | 0.593 |
| Precision | 0.605 | 0.517 | 0.549 | 0.669 |
| Recall | 0.659 | 0.712 | 0.676 | 0.535 |

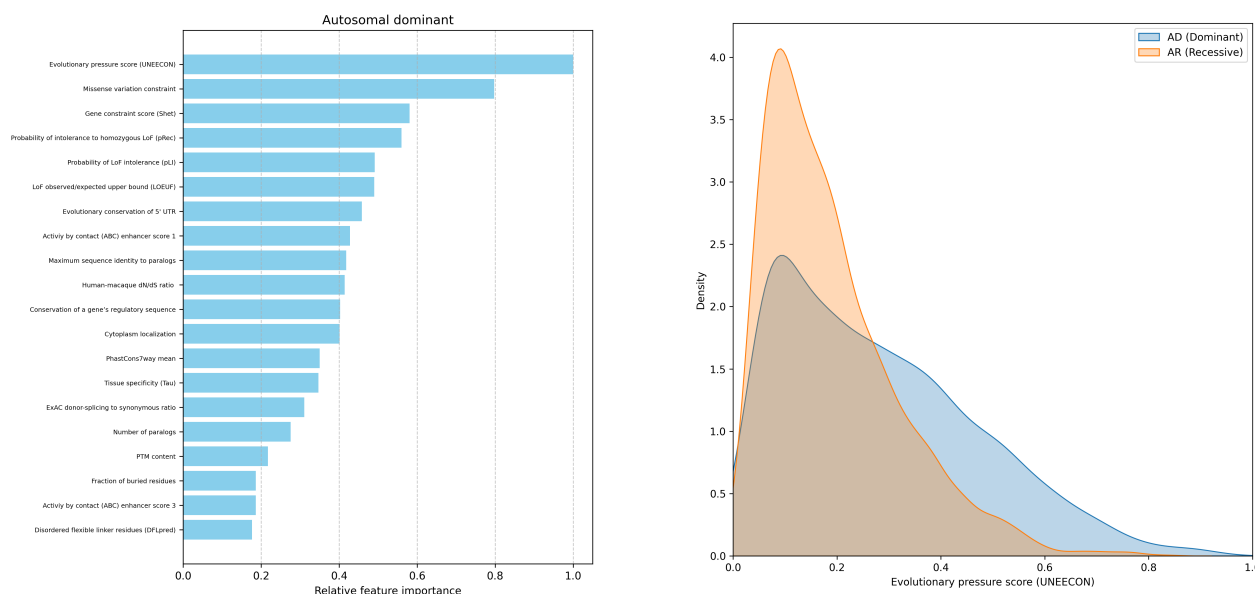


Figure 3: GAT model interpretation for AD prediction (left) and UNEECON score distribution for AD and AR genes (right).

Functional effect feature attribution Using the GCN model, we measured features attribution for correctly predicted DN, HI, and GOF proteins. Because features are at residue-level and prediction are at protein-level, we cannot draw direct conclusions from these measurements, yet they can help to understand the associations.

For DN proteins, the most important feature was the RNA-binding score based on DR-NApred²³ (Figure 5, left). Using the labeled data, we observed that residues in DN proteins have higher RNA-binding scores compared to HI and GOF proteins (Supplementary Figure S1).

For HI proteins, as shown in Figure 5 (middle), topological domain is the strongest predictor. This feature was derived from UniProt²⁴. We observed that HI proteins have a lower fraction of topological domains compared to DN and GOF proteins (Supplementary Figure S2).

Feature attribution analysis for GOF proteins showed that the top feature is the helix structure (Figure 5, right), derived from UniProt²⁴. The distribution of helical fractions indicates that GOF proteins have a relatively higher fraction of helical structures compared to HI and DN proteins (Supplementary Figure S3).

Proteome-wide inference

MOI prediction for all autosomal proteins Of the 17,248 nodes in the PPI network, 16,477 (96%) were autosomal, and we used the GAT model to predict the most likely MOI for all of them. A total of 8,869 (54%) were predicted to be AR, 6,277 (38%) were predicted to be AD, and 1,206 (7%) were predicted to be ADAR (Supplementary Figure S4). As expected, we observed a strong negative correlation between the probability of being AD and AR (Pearson correlation coefficient = -0.95) (Supplementary Figure S5).

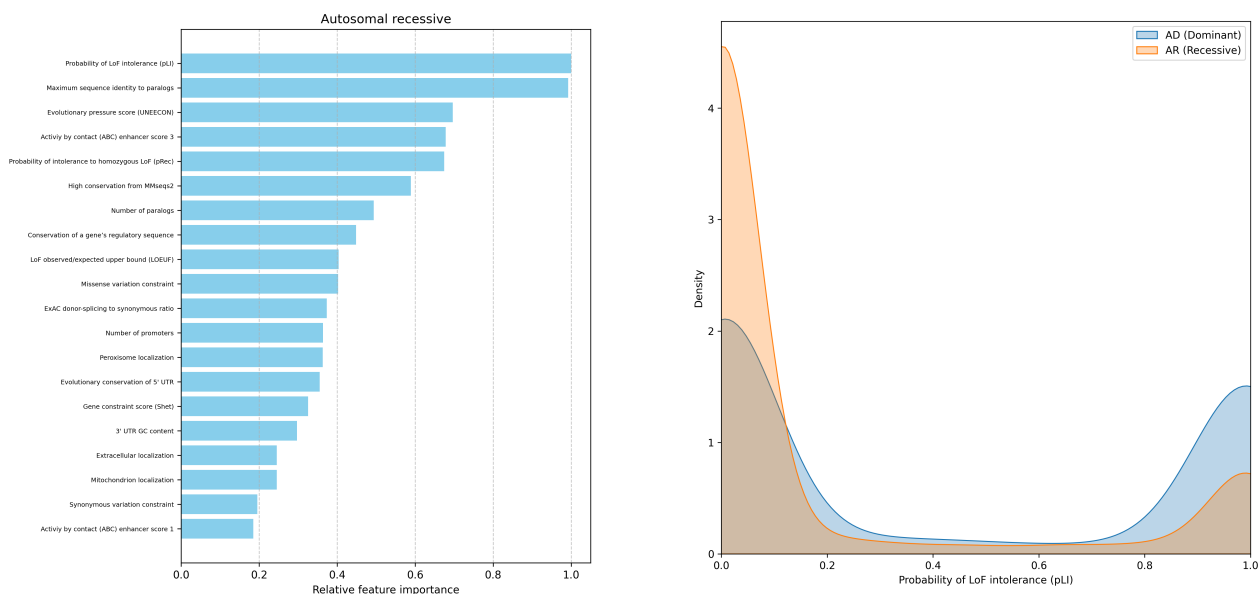


Figure 4: GAT model interpretation for AR prediction (left) and pLI distribution for AD and AR genes (right).

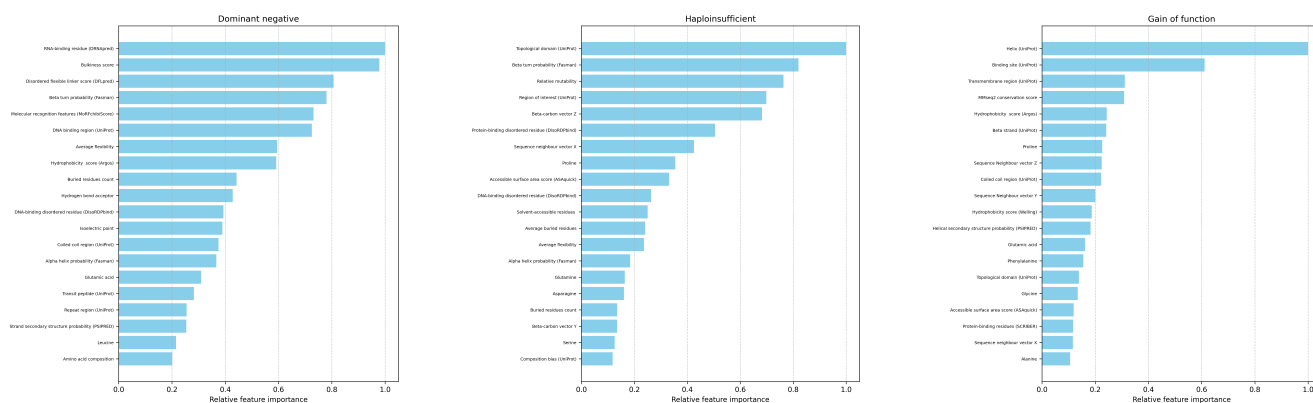


Figure 5: GCN model interpretation for DN (left), HI (middle), and GOF (right) predictions.

Finally, we performed pathway enrichment analyses for AD and AR proteins separately. AD proteins were significantly enriched in pathways associated with gene regulation (Figure 6, left), while AR proteins were significantly overrepresented in mitochondrial pathways (Figure 6, middle). Using the ground truth dataset, we observed that AR proteins are more likely to be localized inside mitochondria compared to AD proteins ($OR = 3.13, CI = [2.47, 3.97]$) (Figure 6, right).

Functional effect prediction for all AD-predicted proteins Based on the proteome-wide MOI predictions, we identified 7,483 AD or ADAR proteins and predicted their functional effect using the GCN model. Among them, 2,043 (28%) were classified as only DN, 1,097 (15%) as only HI, and 415 (6%) as only GOF. Additionally, 1,843 (26%) were both DN and HI, 1,569 (22%) were both DN and GOF, 181 (3%) were both HI and GOF, and 35 (1%) were classified as DN, HI, and GOF (Supplementary Figure S6). We also provide the counts based on AD-only and ADAR-only proteins in Supplementary Figures S7 and S8, respectively.

Pathway enrichment analysis revealed that DN proteins are enriched in pathways associated with filament organization (Figure 7, left), HI proteins are overrepresented in pathways related to transcription regulation (Figure 7, middle), and GOF proteins are enriched in pathways related to ion transport across membranes (Figure 7, right).

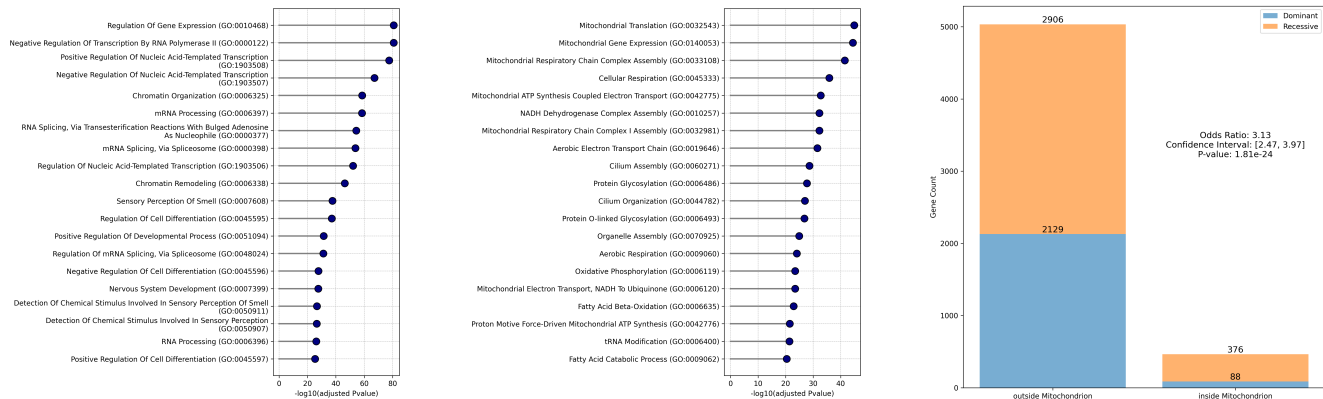


Figure 6: Pathway enrichment analysis for AD (left) and AR (middle) proteins. Right panel shows the number of proteins associated with sub-cellular localization inside or outside mitochondria. The odds ratio was calculated as $\left(\frac{AR_{inside}}{AR_{outside}}\right) / \left(\frac{AD_{inside}}{AD_{outside}}\right)$. P-value was calculated using the Fisher's exact test.

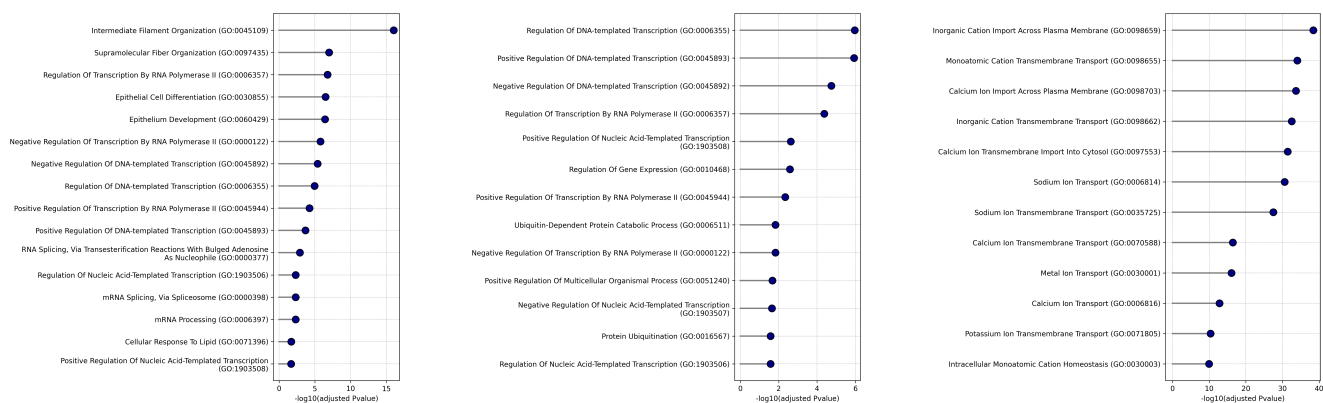


Figure 7: Pathway enrichment analysis for DN (left), HI (middle), and GOF (right) proteins.

DISCUSSION

In this work, we introduce a novel framework that integrates GNNs with structural interactomics to predict both the MOI and the functional effects of mutated proteins in genetic disorders. By leveraging PPI network and high-resolution protein structures, we offer a graph-of-graphs approach that addresses two critical aspects of genetic disease prediction. This allows us to not only classify proteins as AD or AR but also predict whether AD diseases manifest through HI, GOF, or DN mechanisms. Our framework demonstrated good performance in predicting MOI, with the GAT model achieving the best F_1 score for identifying AD and AR proteins. In terms of functional effects, the GCN model effectively classified HI, GOF, and DN proteins based on structural features.

The most important feature in predicting AD proteins is the evolutionary pressure score (UN-ECON)²¹. This aligns with previous studies showing that AD proteins experience stronger negative selection than AR proteins^{25,26}. Additionally, we observed a strong enrichment of AD proteins in pathways related to gene expression regulation. Prior research has shown that transcription factors (TFs) are often dosage-sensitive, particularly haploinsufficient, leading to dominant disease phenotypes^{27,28}. This is consistent with the fact that many human birth defects and neurodevelopmental disorders are caused by mutations in a single copy of TFs and chromatin regulator genes²⁹.

For AR proteins, we found that the pLI (probability of loss-of-function intolerance) index is the most important feature. The pLI index estimates the likelihood that knocking out one copy

of a gene will result in a phenotype²². Low-pLI genes typically exhibit functional redundancy or possess sufficient reserve capacity, allowing heterozygous carriers to remain asymptomatic³⁰. We also observed that AR proteins are enriched in mitochondrial pathways, consistent with previous findings that the vast majority of nuclear-encoded mitochondrial disease genes follow a recessive inheritance pattern³¹. This bias toward recessive inheritance likely arises because defects in energy metabolism generally become pathogenic only when both alleles are disrupted. As long as one allele remains functional, mitochondrial pathways can sustain baseline energy production, preventing deleterious consequences^{32,33}.

Feature attribution analysis revealed that DN proteins are strongly associated with high RNA-binding scores, consistent with the previous observation that DN mutations are enriched in nucleic acid-binding pathways⁸. One possible explanation is that DN mutations often occur at critical interaction sites, such as DNA/RNA-binding interfaces, where they allow the mutant protein to retain its ability to bind partners but disrupt the overall function of the interacting complex. Additionally, we observed an enrichment of DN proteins in pathways related to filament organization. This is likely due to the inherent susceptibility of filamentous and polymeric assemblies to "poisoning" by mutant subunits, which can incorporate into multimers and destabilize the entire structure. A well-documented example is keratin-related disorders, where keratins (type I and II intermediate filament proteins) form an essential cytoskeletal network in epithelial cells. Mutations in keratin genes lead to cell fragility and are inherited in an AD manner, with the mutations exerting their effect through a DN mechanism³⁴.

A depletion in topological domain emerged as the most important feature in predicting HI proteins. According to UniProt, the topological domain annotation defines the subcellular compartment in which each non-membrane region of a membrane-spanning protein is located. Our findings indicate that DN and GOF proteins have a higher fraction of topological domain annotations compared to HI proteins, suggesting that HI genes encode fewer membrane-spanning proteins than DN and GOF genes. This distinction may reflect fundamental differences in the functional roles of these proteins and their sensitivity to dosage effects. Furthermore, HI proteins are significantly enriched in pathways related to transcriptional regulation, consistent with previous findings that transcription factors are frequently dosage-sensitive and particularly prone to haploinsufficiency^{27,28}.

Finally, the most important feature for predicting GOF proteins is helix structure. This finding is consistent with previous reports showing that GOF variants are significantly more likely to occur in alpha helices⁶. We also observed that GOF genes are enriched in pathways related to ion transport across membranes, further supporting the structural-functional link between helices and membrane proteins. A notable example are epilepsy-associated genes: approximately 25% of them encode ion channels, many of which causing epilepsy through a GOF mechanism³⁵. This association is biologically plausible, as many membrane proteins have a core architecture of transmembrane helices, which are critical for gating and transport functions^{36,37}.

Although our approach provides a comprehensive view of inheritance patterns and functional effects, it has several limitations. First, the availability of high-quality structural data for all human proteins remains limited, potentially affecting prediction accuracy³⁸. To ensure uniform coverage, we relied on AlphaFold-predicted structures, which offer high accuracy for well-folded domains but have notable drawbacks. Unlike experimentally resolved structures, AlphaFold does not capture conformational flexibility, ligand interactions, or post-translational modifications, all of which are critical for functional interpretation. Additionally, it is less reliable for intrinsically disordered regions and dynamic protein states, where structural plasticity plays a key role³⁹. Beyond structural considerations, our reliance on existing PPI network data introduces potential biases, as interaction coverage varies across tissues and biological contexts⁴⁰. Furthermore, class imbalance in labeled training data may affect model performance, particularly for underrepresented functional categories. Finally, while our method effectively predicts the functional effects of AD

proteins, it does not extend to other inheritance patterns or interactions influenced by polygenic or epistatic effects⁴¹. 225
226

Moving forward, there are several avenues for expanding this work. Incorporating tissue-specific PPI networks and expression data could improve the precision of our predictions, especially for proteins with context-dependent functions⁴⁰. Additionally, expanding the model to account for more complex inheritance patterns, such as polygenic traits and epistasis, could provide a more comprehensive understanding of genetic disease⁴². Moreover, improving the interpretability of models in biological contexts remains essential to derive more actionable insights from the predictions⁴³. Finally, integrating these predictions with other computational tools and databases could further enhance our understanding of genetic diseases by providing a more holistic view of their underlying mechanisms^{44–48}. 227
228
229
230
231
232
233
234
235

RESOURCE AVAILABILITY 236

Lead contact 237

Requests for further information and resources should be directed to and will be fulfilled by the lead contact, Jacques Fellay (jacques.fellay@epfl.ch). 238
239

Materials availability 240

This study did not generate new materials. 241

Data and code availability 242

The data and code for this study is available here. 243

ACKNOWLEDGMENTS 244

This work was funded by the Swiss National Science Foundation via grant #197721 and by the Swiss State Secretariat for Education, Research and Innovation via contribution to project "UNDINE", SBFJ No. 23.00322. 245
246
247

AUTHOR CONTRIBUTIONS 248

Conceptualization, A.S.; methodology, A.S.; investigation, A.S., and J.F.; writing—original draft, A.S.; writing—review & editing, A.S., and J.F.; funding acquisition, J.F.; supervision, J.F. 249
250

DECLARATION OF INTERESTS 251

The authors declare no competing interests. 252

DECLARATION OF GENERATIVE AI AND AI-ASSISTED TECHNOLOGIES

During the preparation of this work, the authors used GPT-4 in order to improve writing and readability.

SUPPLEMENTAL INFORMATION INDEX

Table S1. The descriptions of protein features. 258

Table S2. The descriptions of amino acid features. 259

Table S3. Hyperparameter tuning results for the MOI prediction model. 260

Table S4. Hyperparameter tuning results for the functional effect prediction model. 261

Table S5. Prediction of MOI for all autosomal proteins. 262

Table S6. Prediction of functional effect for all AD-predicted proteins. 263

Figure S1: Distribution of RNA-binding scores based on DRNAPred. 264

Figure S2: The distribution of the fraction of topological domain based on UniProt annotations. 265

Figure S3: The distribution of the fraction of helical residues based on UniProt annotations. 266

Figure S4: Number of AD, AR, and ADAR predicted based on the selected GAT model. 267

Figure S5: probability of AD (pAD) vs probability of AR (pAR) for all autosomal proteins. 268

Figure S6: Number of proteins predicted based on the selected GCN model. Prediction was performed on all AD and ADAR proteins. 269
270

Figure S7: Number of proteins predicted based on the selected GCN model. ADAR proteins were excluded for this calculation. 271
272

Figure S8: Number of proteins predicted based on the selected GCN model. Only ADAR proteins were included for this calculation. 273
274

References

1. Zschocke, J., Byers, P. H., and Wilkie, A. O. M. (2023). Mendelian inheritance revisited: dominance and recessiveness in medical genetics. *Nat. Rev. Genet.* *24*, 442–463. 275
276
277
2. Veitia, R. A. (2002). Exploring the etiology of haploinsufficiency. *Bioessays* *24*, 175–184. 278
3. Backwell, L., and Marsh, J. A. (2022). Diverse molecular mechanisms underlying pathogenic protein mutations: Beyond the loss-of-function paradigm. *Annu. Rev. Genomics Hum. Genet.* *23*, 475–498. 279
280
281
4. Quinodoz, M., Royer-Bertrand, B., Cisarova, K., Di Gioia, S. A., Superti-Furga, A., and Rivolta, C. (2017). DOMINO: Using machine learning to predict genes associated with dominant disorders. *Am. J. Hum. Genet.* *101*, 623–629. 282
283
284
5. Petrazzini, B. O., Balick, D. J., Forrest, I. S., Cho, J., Rocheleau, G., Jordan, D. M., and Do, R. (2024). Ensemble and consensus approaches to prediction of recessive inheritance for missense variants in human disease. *Cell Rep. Methods* *4*, 100914. 285
286
287
6. Stein, D., Kars, M. E., Wu, Y., Bayrak, Ç. S., Stenson, P. D., Cooper, D. N., Schlessinger, A., and Itan, Y. (2023). Genome-wide prediction of pathogenic gain- and loss-of-function variants from ensemble learning of a diverse feature set. *Genome Med.* *15*, 103. 288
289
290
7. Gerasimavicius, L., Livesey, B. J., and Marsh, J. A. (2022). Loss-of-function, gain-of-function and dominant-negative mutations have profoundly different effects on protein structure. *Nat. Commun.* *13*, 3895. 291
292
293
8. Badonyi, M., and Marsh, J. A. (2024). Proteome-scale prediction of molecular mechanisms underlying dominant genetic diseases. *PLOS ONE* *19*, e0307312. URL: <http://dx.doi.org/10.1371/journal.pone.0307312>. doi:10.1371/journal.pone.0307312. 294
295
296
9. Zhou, J., Cui, G., Hu, S., Zhang, Z., Yang, C., Liu, Z., Wang, L., Li, C., and Sun, M. (2021). Graph neural networks: A review of methods and applications. URL: <https://arxiv.org/abs/1812.08434>. arXiv:1812.08434. 297
298
299
10. D’Agostino, G., and Scala, A., eds. *Networks of networks: The last frontier of complexity. Understanding complex systems* Cham, Switzerland: Springer International Publishing (2014). 300
301
302
11. Szklarczyk, D., Kirsch, R., Koutrouli, M., Nastou, K., Mehryary, F., Hachilif, R., Gable, A. L., Fang, T., Doncheva, N., Pyysalo, S., Bork, P., Jensen, L., and von Mering, C. (2022). The string database in 2023: protein–protein association networks and functional enrichment analyses for any sequenced genome of interest. *Nucleic Acids Research* *51*, D638–D646. URL: <http://dx.doi.org/10.1093/nar/gkac1000>. doi:10.1093/nar/gkac1000. 303
304
305
306
307
12. Oughtred, R., Rust, J., Chang, C., Breitkreutz, B., Stark, C., Willems, A., Boucher, L., Leung, G., Kolas, N., Zhang, F., Dolma, S., Coulombe-Huntington, J., Chatr-aryamontri, A., Dolinski, K., and Tyers, M. (2020). The `ijscpi` database: A comprehensive biomedical resource of curated protein, genetic, and chemical interactions. *Protein Science* *30*, 187–200. URL: <http://dx.doi.org/10.1002/pro.3978>. doi:10.1002/pro.3978. 308
309
310
311
312
13. Luck, K., Kim, D.-K., Lambourne, L., Spirohn, K., Begg, B. E., Bian, W., Brignall, R., Cafarelli, T., Campos-Laborie, F. J., Charlotteaux, B., Choi, D., Coté, A. G., Daley, M., Deimling, S., Desbuleux, A., Dricot, A., Gebbia, M., Hardy, M. F., Kishore, N., Knapp, J. J., 313
314
315

- Kovács, I. A., Lemmens, I., Mee, M. W., Mellor, J. C., Pollis, C., Pons, C., Richardson, A. D., Schlabach, S., Teeking, B., Yadav, A., Babor, M., Balcha, D., Basha, O., Bowman-Colin, C., Chin, S.-F., Choi, S. G., Colabella, C., Coppin, G., D'Amata, C., De Ridder, D., De Rouck, S., Duran-Frigola, M., Ennajdaoui, H., Goebels, F., Goehring, L., Gopal, A., Haddad, G., Hatchi, E., Helmy, M., Jacob, Y., Kassa, Y., Landini, S., Li, R., van Lieshout, N., MacWilliams, A., Markey, D., Paulson, J. N., Rangarajan, S., Rasla, J., Rayhan, A., Rolland, T., San-Miguel, A., Shen, Y., Sheykhkarimli, D., Sheynkman, G. M., Simonovsky, E., Taşan, M., Tejada, A., Tropepe, V., Twizere, J.-C., Wang, Y., Weatheritt, R. J., Weile, J., Xia, Y., Yang, X., Yeger-Lotem, E., Zhong, Q., Aloy, P., Bader, G. D., De Las Rivas, J., Gaudet, S., Hao, T., Rak, J., Tavernier, J., Hill, D. E., Vidal, M., Roth, F. P., and Calderwood, M. A. (2020). A reference map of the human binary protein interactome. *Nature* *580*, 402–408. URL: <http://dx.doi.org/10.1038/s41586-020-2188-x>. doi:10.1038/s41586-020-2188-x.
14. Menche, J., Sharma, A., Kitsak, M., Ghiassian, S. D., Vidal, M., Loscalzo, J., and Barabási, A.-L. (2015). Uncovering disease-disease relationships through the incomplete interactome. *Science* *347*. URL: <http://dx.doi.org/10.1126/science.1257601>. doi:10.1126/science.1257601.
15. Varadi, M., Bertoni, D., Magana, P., Paramval, U., Pidruchna, I., Radhakrishnan, M., Tsenkov, M., Nair, S., Mirdita, M., Yeo, J., Kovalevskiy, O., Tunyasuvunakool, K., Laydon, A., Židek, A., Tomlinson, H., Hariharan, D., Abrahamson, J., Green, T., Jumper, J., Birney, E., Steinegger, M., Hassabis, D., and Velankar, S. (2023). AlphaFold protein structure database in 2024: providing structure coverage for over 214 million protein sequences. *Nucleic Acids Research* *52*, D368–D375. URL: <http://dx.doi.org/10.1093/nar/gkad1011>. doi:10.1093/nar/gkad1011.
16. Jamasb, A. R., Torné, R. V., Ma, E. J., Du, Y., Harris, C., Huang, K., Hall, D., Lio, P., and Blundell, T. L. (2022). Graphein - a python library for geometric deep learning and network analysis on biomolecular structures and interaction networks. In: Oh, A. H., Agarwal, A., Belgrave, D., and Cho, K., eds. *Advances in Neural Information Processing Systems*. URL: <https://openreview.net/forum?id=9xRZlV6Gf0X>.
17. Kipf, T. N., and Welling, M. (2017). Semi-supervised classification with graph convolutional networks. URL: <https://arxiv.org/abs/1609.02907>. arXiv:1609.02907.
18. Brody, S., Alon, U., and Yahav, E. (2022). How attentive are graph attention networks? URL: <https://arxiv.org/abs/2105.14491>. arXiv:2105.14491.
19. Xu, K., Hu, W., Leskovec, J., and Jegelka, S. (2019). How powerful are graph neural networks? URL: <https://arxiv.org/abs/1810.00826>. arXiv:1810.00826.
20. Steinegger, M., and Söding, J. (2017). Mmseqs2 enables sensitive protein sequence searching for the analysis of massive data sets. *Nature Biotechnology* *35*, 1026–1028. URL: <http://dx.doi.org/10.1038/nbt.3988>. doi:10.1038/nbt.3988.
21. Huang, Y.-F. (2020). Unified inference of missense variant effects and gene constraints in the human genome. *PLoS Genet.* *16*, e1008922.
22. Lek, M., Karczewski, K. J., Minikel, E. V., Samocha, K. E., Banks, E., Fennell, T., O'Donnell-Luria, A. H., Ware, J. S., Hill, A. J., Cummings, B. B., Tukiainen, T., Birnbaum, D. P., Kosmicki, J. A., Duncan, L. E., Estrada, K., Zhao, F., Zou, J., Pierce-Hoffman, E., Berghout, J., Cooper, D. N., DeFlaux, N., DePristo, M., Do, R., Flannick, J., Fromer, M., Gauthier, L., Goldstein, J., Gupta, N., Howrigan, D., Kiezun, A., Kurki, M. I., Moonshine, A. L., Natarajan,

- P., Orozco, L., Peloso, G. M., Poplin, R., Rivas, M. A., Ruano-Rubio, V., Rose, S. A., Ruderfer, D. M., Shakir, K., Stenson, P. D., Stevens, C., Thomas, B. P., Tiao, G., Tusie-Luna, M. T., Weisburd, B., Won, H.-H., Yu, D., Altshuler, D. M., Ardissino, D., Boehnke, M., Danesh, J., Donnelly, S., Elosua, R., Florez, J. C., Gabriel, S. B., Getz, G., Glatt, S. J., Hultman, C. M., Kathiresan, S., Laakso, M., McCarroll, S., McCarthy, M. I., McGovern, D., McPherson, R., Neale, B. M., Palotie, A., Purcell, S. M., Saleheen, D., Scharf, J. M., Sklar, P., Sullivan, P. F., Tuomilehto, J., Tsuang, M. T., Watkins, H. C., Wilson, J. G., Daly, M. J., and MacArthur, D. G. (2016). Analysis of protein-coding genetic variation in 60, 706 humans. *Nature* *536*, 285–291. URL: <http://dx.doi.org/10.1038/nature19057>. doi:10.1038/nature19057.
23. Yan, J., and Kurgan, L. (2017). DRNAPred, fast sequence-based method that accurately predicts and discriminates DNA- and RNA-binding residues. *Nucleic Acids Res.* (gkx059).
24. Bateman, A., Martin, M.-J., Orchard, S., Magrane, M., Ahmad, S., Alpi, E., Bowler-Barnett, E. H., Britto, R., Bye-A-Jee, H., Cukura, A., Denny, P., Dogan, T., Ebenezer, T., Fan, J., Garmiri, P., da Costa Gonzales, L. J., Hatton-Ellis, E., Hussein, A., Ignatchenko, A., Insana, G., Ishtiaq, R., Joshi, V., Jyothi, D., Kandasaamy, S., Lock, A., Luciani, A., Lugaric, M., Luo, J., Lussi, Y., MacDougall, A., Madeira, F., Mahmoudy, M., Mishra, A., Moulang, K., Nightingale, A., Pundir, S., Qi, G., Raj, S., Raposo, P., Rice, D. L., Saidi, R., Santos, R., Speretta, E., Stephenson, J., Tootoo, P., Turner, E., Tyagi, N., Vasudev, P., Warner, K., Watkins, X., Zaru, R., Zellner, H., Bridge, A. J., Aimo, L., Argoud-Puy, G., Auchincloss, A. H., Axelsen, K. B., Bansal, P., Baratin, D., Batista Neto, T. M., Blatter, M.-C., Bolleman, J. T., Boutet, E., Breuza, L., Gil, B. C., Casals-Casas, C., Echioukh, K. C., Coudert, E., Cuhe, B., de Castro, E., Estreicher, A., Famiglietti, M. L., Feuermann, M., Gasteiger, E., Gaudet, P., Gehant, S., Gerritsen, V., Gos, A., Gruaz, N., Hulo, C., Hyka-Nouspikel, N., Jungo, F., Kerhornou, A., Le Mercier, P., Lieberherr, D., Masson, P., Morgat, A., Muthukrishnan, V., Paesano, S., Pedruzzi, I., Pilbout, S., Pourcel, L., Poux, S., Pozzato, M., Pruess, M., Redaschi, N., Rivoire, C., Sigrist, C. J. A., Sonesson, K. et al. (2022). Uniprot: the universal protein knowledgebase in 2023. *Nucleic Acids Research* *51*, D523–D531. URL: <http://dx.doi.org/10.1093/nar/gkac1052>. doi:10.1093/nar/gkac1052.
25. Blekhman, R., Man, O., Herrmann, L., Boyko, A. R., Indap, A., Kosiol, C., Bustamante, C. D., Teshima, K. M., and Przeworski, M. (2008). Natural selection on genes that underlie human disease susceptibility. *Curr. Biol.* *18*, 883–889.
26. Rapaport, F., Boisson, B., Gregor, A., Béziat, V., Boisson-Dupuis, S., Bustamante, J., Jouanguy, E., Puel, A., Rosain, J., Zhang, Q., Zhang, S.-Y., Gleeson, J. G., Quintana-Murci, L., Casanova, J.-L., Abel, L., and Patin, E. (2021). Negative selection on human genes underlying inborn errors depends on disease outcome and both the mode and mechanism of inheritance. *Proc. Natl. Acad. Sci. U. S. A.* *118*, e2001248118.
27. Seidman, J. G., and Seidman, C. (2002). Transcription factor haploinsufficiency: when half a loaf is not enough. *J. Clin. Invest.* *109*, 451–455.
28. van der Lee, R., Correard, S., and Wasserman, W. W. (2020). Deregulated regulators: Disease-causing cis variants in transcription factor genes. *Trends Genet.* *36*, 523–539.
29. Zug, R. (2022). Developmental disorders caused by haploinsufficiency of transcriptional regulators: a perspective based on cell fate determination. *Biol. Open* *11*.
30. Huang, N., Lee, I., Marcotte, E. M., and Hurles, M. E. (2010). Characterising and predicting haploinsufficiency in the human genome. *PLoS Genet.* *6*, e1001154.

31. Gusic, M., and Prokisch, H. (2021). Genetic basis of mitochondrial diseases. *FEBS Lett.* 595, 1132–1158. 404
405
32. Kacser, H., and Burns, J. A. (1981). The molecular basis of dominance. *Genetics* 97, 639–666. 406
407
33. Deutschbauer, A. M., Jaramillo, D. F., Proctor, M., Kumm, J., Hillenmeyer, M. E., Davis, R. W., Nislow, C., and Giaever, G. (2005). Mechanisms of haploinsufficiency revealed by genome-wide profiling in yeast. *Genetics* 169, 1915–1925. 408
409
410
34. Smith, F. (2003). The molecular genetics of keratin disorders. *Am. J. Clin. Dermatol.* 4, 347–364. 411
412
35. Oyrer, J., Maljevic, S., Scheffer, I. E., Berkovic, S. F., Petrou, S., and Reid, C. A. (2018). Ion channels in genetic epilepsy: From genes and mechanisms to disease-targeted therapies. *Pharmacol. Rev.* 70, 142–173. 413
414
415
36. Sansom, M. S. (2000). Potassium channels: watching a voltage-sensor tilt and twist. *Curr. Biol.* 10, R206–9. 416
417
37. Fernández-Quintero, M. L., El Ghaleb, Y., Tuluc, P., Campiglio, M., Liedl, K. R., and Flucher, B. E. (2021). Structural determinants of voltage-gating properties in calcium channels. *Elife* 10. 418
419
420
38. Bertoline, L. M. F., Lima, A. N., Krieger, J. E., and Teixeira, S. K. (2023). Before and after AlphaFold2: An overview of protein structure prediction. *Front. Bioinform.* 3, 1120370. 421
422
39. Perrakis, A., and Sixma, T. K. (2021). AI revolutions in biology: The joys and perils of AlphaFold. *EMBO Rep.* 22, e54046. 423
424
40. Ziv, M., Gruber, G., Sharon, M., Vinogradov, E., and Yeger-Lotem, E. (2022). The TissueNet v.3 database: Protein-protein interactions in adult and embryonic human tissue contexts. *J. Mol. Biol.* 434, 167532. 425
426
427
41. Phillips, P. C. (2008). Epistasis—the essential role of gene interactions in the structure and evolution of genetic systems. *Nat. Rev. Genet.* 9, 855–867. 428
429
42. Boyle, E. A., Li, Y. I., and Pritchard, J. K. (2017). An expanded view of complex traits: From polygenic to omnigenic. *Cell* 169, 1177–1186. 430
431
43. Chen, V., Yang, M., Cui, W., Kim, J. S., Talwalkar, A., and Ma, J. (2024). Applying interpretable machine learning in computational biology-pitfalls, recommendations and opportunities for new developments. *Nat. Methods* 21, 1454–1461. 432
433
434
44. Saadat, A., and Fellay, J. (2024). DNA language model and interpretable graph neural network identify genes and pathways involved in rare diseases. In: Edwards, C., Wang, Q., Li, M., Zhao, L., Hope, T., and Ji, H., eds. *Proceedings of the 1st Workshop on Language + Molecules (L+M 2024)*. Bangkok, Thailand: Association for Computational Linguistics (103–115). URL: <https://aclanthology.org/2024.langmol-1.13/>. doi:10.18653/v1/2024.langmol-1.13. 435
436
437
438
439
440
45. Saadat, A., and Fellay, J. (2025). From mutation to degradation: Predicting nonsense-mediated decay with NMDEP. *arXiv:2502.14547*. 441
442

46. Saadat, A., and Fellay, J. (2024). Fine-tuning the esm2 protein language model to understand the functional impact of missense variants. URL: <https://arxiv.org/abs/2410.10919>. arXiv:2410.10919. 443
444
445
47. Saadat, A., and Fellay, J. (2025). Exploring the potential of zygosity and genetic variation in DNA language models. In: ICLR 2025 Workshop on Machine Learning for Genomics Explorations. URL: <https://openreview.net/forum?id=wW6jhSMTEg>. 446
447
448
48. Ruiz, P. R., Saadat, A., Tran, T. T., Smedt, O. M., Zhang, P., and Fellay, J. (2025). Benchmarking fine-tuned RNA language models for branch point prediction. In: ICLR 2025 Workshop on Machine Learning for Genomics Explorations. URL: <https://openreview.net/forum?id=Q15Dg5lQou>. 449
450
451
452
49. DiStefano, M. T., Goehringer, S., Babb, L., Alkuraya, F. S., Amberger, J., Amin, M., Austin-Tse, C., Balzotti, M., Berg, J. S., Birney, E., Bocchini, C., Bruford, E. A., Coffey, A. J., Collins, H., Cunningham, F., Daugherty, L. C., Einhorn, Y., Firth, H. V., Fitzpatrick, D. R., Foulger, R. E., Goldstein, J., Hamosh, A., Hurles, M. R., Leigh, S. E., Leong, I. U., Maddirevula, S., Martin, C. L., McDonagh, E. M., Olry, A., Puzriakova, A., Radtke, K., Ramos, E. M., Rath, A., Riggs, E. R., Roberts, A. M., Rodwell, C., Snow, C., Stark, Z., Tahiliani, J., Tweedie, S., Ware, J. S., Weller, P., Williams, E., Wright, C. F., Yates, T. M., and Rehm, H. L. (2022). The gene curation coalition: A global effort to harmonize gene–disease evidence resources. *Genetics in Medicine* 24, 1732–1742. URL: <http://dx.doi.org/10.1016/j.gim.2022.04.017>. doi:10.1016/j.gim.2022.04.017. 453
454
455
456
457
458
459
460
461
462
50. Hamosh, A. (2002). Online mendelian inheritance in man (omim), a knowledgebase of human genes and genetic disorders. *Nucleic Acids Research* 30, 52–55. URL: <http://dx.doi.org/10.1093/nar/30.1.52>. doi:10.1093/nar/30.1.52. 463
464
465
51. Fey, M., and Lenssen, J. E. (2019). Fast graph representation learning with pytorch geometric. URL: <https://arxiv.org/abs/1903.02428>. arXiv:1903.02428. 466
467
52. Khemani, B., Patil, S., Kotecha, K., and Tanwar, S. (2024). A review of graph neural networks: concepts, architectures, techniques, challenges, datasets, applications, and future directions. *J. Big Data* 11. 468
469
470
53. Kingma, D. P., and Ba, J. (2014). Adam: A method for stochastic optimization. arXiv:1412.6980. 471
472
54. Sundararajan, M., Taly, A., and Yan, Q. (2017). Axiomatic attribution for deep networks. URL: <https://arxiv.org/abs/1703.01365>. arXiv:1703.01365. 473
474
55. Kokhlikyan, N., Miglani, V., Martin, M., Wang, E., Alsallakh, B., Reynolds, J., Melnikov, A., Kliushkina, N., Araya, C., Yan, S., and Reblitz-Richardson, O. (2020). Captum: A unified and generic model interpretability library for pytorch. arXiv:2009.07896. 475
476
477
56. Fang, Z., Liu, X., and Peltz, G. (2022). Gseapy: a comprehensive package for performing gene set enrichment analysis in python. *Bioinformatics* 39. URL: <http://dx.doi.org/10.1093/bioinformatics/btac757>. doi:10.1093/bioinformatics/btac757. 478
479
480
57. Khatri, P., Sirota, M., and Butte, A. J. (2012). Ten years of pathway analysis: Current approaches and outstanding challenges. *PLoS Computational Biology* 8, e1002375. URL: <http://dx.doi.org/10.1371/journal.pcbi.1002375>. doi:10.1371/journal.pcbi.1002375. 481
482
483
484

58. Ashburner, M., Ball, C. A., Blake, J. A., Botstein, D., Butler, H., Cherry, J. M., Davis, A. P., Dolinski, K., Dwight, S. S., Eppig, J. T., Harris, M. A., Hill, D. P., Issel-Tarver, L., Kasarskis, A., Lewis, S., Matese, J. C., Richardson, J. E., Ringwald, M., Rubin, G. M., and Sherlock, G. (2000). Gene ontology: tool for the unification of biology. *Nature Genetics* 25, 25–29. URL: <http://dx.doi.org/10.1038/75556>. doi:10.1038/75556. 485
486
487
488
489
59. Aleksander, S. A., Balhoff, J., Carbon, S., Cherry, J. M., Drabkin, H. J., Ebert, D., Feuer- 490
mann, M., Gaudet, P., Harris, N. L., Hill, D. P., Lee, R., Mi, H., Moxon, S., Mungall, C. J., 491
Muruganugan, A., Mushayahama, T., Sternberg, P. W., Thomas, P. D., Van Auken, K., Ram- 492
sey, J., Siegele, D. A., Chisholm, R. L., Fey, P., Aspromonte, M. C., Nugnes, M. V., Quaglia, 493
F., Tosatto, S., Giglio, M., Nadendla, S., Antonazzo, G., Attrill, H., dos Santos, G., Mary- 494
gold, S., Strelets, V., Tabone, C. J., Thurmond, J., Zhou, P., Ahmed, S. H., Asanithong, 495
P., Luna Buitrago, D., Erdol, M. N., Gage, M. C., Ali Kadhum, M., Li, K. Y. C., Long, M., 496
Michalak, A., Pesala, A., Pritazahra, A., Saverimuttu, S. C. C., Su, R., Thurlow, K. E., 497
Lovering, R. C., Logie, C., Oliferenko, S., Blake, J., Christie, K., Corbani, L., Dolan, M. E., 498
Drabkin, H. J., Hill, D. P., Ni, L., Sitnikov, D., Smith, C., Cuzick, A., Seager, J., Cooper, L., 499
Elser, J., Jaiswal, P., Gupta, P., Jaiswal, P., Naithani, S., Lera-Ramirez, M., Rutherford, K., 500
Wood, V., De Pons, J. L., Dwinell, M. R., Hayman, G. T., Kaldunski, M. L., Kwitek, A. E., 501
Laulederkind, S. J. F., Tutaj, M. A., Vedi, M., Wang, S.-J., D'Eustachio, P., Aimò, L., Axelsen, 502
K., Bridge, A., Hyka-Nouspikel, N., Morgat, A., Aleksander, S. A., Cherry, J. M., Engel, 503
S. R., Karra, K., Miyasato, S. R., Nash, R. S., Skrzypek, M. S., Weng, S., Wong, E. D., 504
Bakker, E. et al. (2023). The gene ontology knowledgebase in 2023. *GENETICS* 224. URL: 505
<http://dx.doi.org/10.1093/genetics/iyad031>. doi:10.1093/genetics/iyad031. 506

STAR METHODS

507

Data collection

508

Mode of inheritance We collected the MOI data from the Gene Curation Coalition (GenCC)⁴⁹ as well as the Online Mendelian Inheritance in Man (OMIM)⁵⁰. For GenCC records, we kept records with definitive, strong, or moderate gene-disease clinical validity. We focused on autosomal proteins, due to intrinsic differences in MOI for X chromosome proteins. Proteins were accordingly labeled as AD, AR, or ADAR (both dominant and recessive).

509

510

511

512

513

Molecular mechanism We collected the functional effect of AD proteins from Badonyi and Marsh⁸. This is a curated set of AD proteins labeled with their known functional effects, including DN, GOF, and HI.

514

515

516

PPI network To make a comprehensive PPI network, we combined the interaction from four resources: STRINGdb with interaction score ≥ 0.7 ¹¹, BioGRID¹², the Human Reference Interactome (HuRI)¹³, and Menche et al.¹⁴, which resulted in a network with 17,248 nodes, and 375,494 edges.

517

518

519

520

Protein graph We downloaded the predicted structures of all human proteins from the AlphaFold database¹⁵. We then used Graphein¹⁶ to construct a residue graph for each protein based on its structure. In these residue graphs, nodes represent amino acids, and edges capture various interactions between them, including peptide bonds, aromatic interactions, hydrogen bonds, disulfide bonds, ionic interactions, aromatic-sulfur interactions, and cation- π interactions. To account for long-range amino acid interactions, we included edges between amino acids that are spatially close (<5 angstroms) but distant in the sequence (>5 amino acids apart).

521

522

523

524

525

526

527

Protein features We annotated all proteins with 97 features covering various aspects of protein characteristics, including structure and function, conservation and constraint, and expression and regulation. Using the training set, we excluded features with low variance (<0.1) or high correlation (>0.8), resulting in a final selection of 78 features. The complete list of initial and selected protein features is provided in Supplementary Table 1.

528

529

530

531

532

Residue features For the residue graphs, we annotated the nodes (i.e. amino acids) with 132 features covering various aspects including structure and function, sequence, biochemical, and evolutionary characteristics. Using the training set, we excluded features with low variance (<0.01) or high correlation (>0.8), resulting in a final selection of 73 features. The complete list of initial and selected residue features is provided in Supplementary Table 2.

533

534

535

536

537

Model development

538

Study design In this study, MOI is predicted by classifying nodes in a PPI network, while functional effect prediction is framed as a graph classification task. Both models use a multi-label classification approach, allowing inputs to have more than one label. All experiments were conducted using the PyTorch Geometric library⁵¹.

539

540

541

542

We leverage GNNs because they can directly utilize the relational structure of the data by propagating information through the graph⁵², whereas traditional machine learning models require explicit feature engineering to incorporate graph-based information. For MOI prediction,

543

544

545

PPI networks encode valuable topological properties that influence disease mechanisms. GNNs capture both individual protein features and their connectivity within the network, an aspect that conventional ML models struggle to integrate effectively. Similarly, for functional effect prediction, protein structure graphs provide spatial and biochemical context at the residue level. While traditional ML approaches require manually extracting graph-based features (e.g., graph centrality, residue connectivity), GNNs inherently integrate these properties, enabling a more comprehensive representation of structural and functional information.

Architecture For both MOI and functional effect prediction, we utilized various graph neural network architecture including graph convolutional network (GCN)¹⁷, graph attention network (GAT)¹⁸, and graph isomorphism network (GIN)¹⁹.

GCNs extend the concept of convolution from grid-like data (such as images) to graph data, allowing the aggregation of feature information from neighboring nodes. This approach effectively captures local graph structure and node features. The forward propagation formula in a GCN is given by:

$$h_i^{(l+1)} = \sum_{j \in \mathcal{N}(i)} \frac{1}{\sqrt{\deg(i)}\sqrt{\deg(j)}} \mathbf{W}^{(l)} h_j^{(l)}$$

- $h_j^{(l)}$: The node feature vector at layer l .
- $h_i^{(l+1)}$: The updated node feature vector at layer $l + 1$.
- $\mathbf{W}^{(l)}$: The learnable weight matrix for layer l .
- $\mathcal{N}(i)$: The set of neighbors of node i (including itself due to the self-loop).
- $\frac{1}{\sqrt{\deg(i)}\sqrt{\deg(j)}}$: The normalization term based on the degrees of nodes i and j , ensuring that nodes with different degrees contribute proportionally to the update.

GINs are designed to be powerful for graph isomorphism, making them capable of distinguishing a wide variety of graph structures. They achieve this by using a multi-layer perceptron (MLP) to aggregate node features, enhancing their discriminative power. The update rule for the GIN is given by:

$$h_i^{(l+1)} = \text{MLP}^{(l)} \left((1 + \epsilon^{(l)}) h_i^{(l)} + \sum_{j \in \mathcal{N}(i)} h_j^{(l)} \right)$$

- $h_i^{(l)}$: The node feature vector at layer l .
- $h_i^{(l+1)}$: The updated node feature vector at layer $l + 1$.
- $\text{MLP}^{(l)}$: A multi-layer perceptron applied at layer l , which acts as a learnable transformation function on the aggregated node features.
- $\epsilon^{(l)}$: A learnable parameter at layer l that adjusts the contribution of the central node's own features $h_i^{(l)}$.
- $\mathcal{N}(i)$: The set of neighbors of node i . The sum $\sum_{j \in \mathcal{N}(i)} h_j^{(l)}$ aggregates the features of all neighbor nodes in layer l .

GATs introduce attention mechanisms to GNNs, enabling nodes to assign different importance weights to their neighbors. This allows for more flexible and expressive feature aggregation, potentially improving performance on tasks where certain neighbors have more influence than others. The forward propagation rule for GAT is given by:

$$h_i^{(l+1)} = \sigma \left(\sum_{j \in \mathcal{N}(i)} \alpha_{ij}^{(l)} \mathbf{W}^{(l)} h_j^{(l)} \right)$$

$$\alpha_{ij}^{(l)} = \frac{\exp \left(\text{LeakyReLU} \left(a^T \left[\mathbf{W}^{(l)} (h_i^{(l)} \parallel h_j^{(l)}) \right] \right) \right)}{\sum_{k \in \mathcal{N}(i)} \exp \left(\text{LeakyReLU} \left(a^T \left[\mathbf{W}^{(l)} (h_i^{(l)} \parallel h_k^{(l)}) \right] \right) \right)}$$

- $h_i^{(l)}$: The node feature vector at layer l .
- $h_i^{(l+1)}$: The updated node feature vector at layer $l + 1$.
- $\alpha_{ij}^{(l)}$: The attention coefficient between nodes i and j .
- $\mathbf{W}^{(l)}$: The weight matrix at layer l .
- a : The learnable attention vector.
- \parallel : The concatenation operator.
- $\mathcal{N}(i)$: The set of neighbors of node i .
- $\sigma(\cdot)$: A non-linear activation function (ReLU in our implementation).

Hyperparameters In all models, we employed a single hidden layer, with the output layer comprising two units for MOI prediction (AD and AR) and three units for functional effect prediction (DN, HI, and GOF). To identify optimal configurations, for each model we evaluated 25 combinations of hyperparameters, varying the hidden layer size across five values (128, 64, 32, 16, and 8) and the learning rate across five values (ranging from 10^{-2} to 5×10^{-4}). The results of hyperparameter tuning for MOI and functional effect prediction are available in Supplementary Tables 3 and 4, respectively.

Other hyperparameters were set to commonly used values, including a weight decay of 5×10^{-4} and a dropout rate of 0.3. For optimization, we employed the Adam optimizer⁵³ with an adaptive learning rate scheduler (ReduceLRonPlateau), which dynamically adjusted the learning rate based on validation loss.

Training and evaluation To create train, validation, and test splits, we clustered protein sequences using MMseqs2²⁰ with thresholds of 20% coverage and 20% sequence identity. For each model, the proteins were divided into 80% training, 10% validation, and 10% testing sets, ensuring minimal data leakage by performing the splits at the cluster level.

We trained each model using a binary cross entropy loss for maximum 100 epochs and used early stopping based on validation loss to avoid over-fitting. We evaluated each selected model on the unseen test data using F_1 , precision, and recall scores.

We benchmarked the performance of our model against previous state-of-the-art approaches. For MOI prediction, we compared our model with DOMINO⁴, which predicts the probability of a protein's association with dominant disorders (pAD). We used our MOI test set and excluded

any proteins present in DOMINO's training data. Since no threshold was provided, we classified proteins as AD if $pAD > 0.6$, AR if $pAD < 0.4$, and ADAR otherwise.

For functional effect prediction, we compared our model with those from Badonyi and Marsh⁸, which include three separate SVM classifiers: DN vs. LOF, GOF vs. LOF, and LOF vs. non-LOF. To evaluate performance in a multi-label classification setting, we combined the test sets from these models and utilized the pre-calculated probabilities. We did not benchmark against other traditional ML models, as Badonyi and Marsh⁸ had already compared multiple approaches including SVM, LightGBM, Random Forest, Logistic Regression, and MLP, and identified SVM as the best performer. Based on these findings, we focused our comparisons on the strongest traditional baseline.

Model explanation To study the importance of features, we utilized Integrated Gradients⁵⁴ using Captum⁵⁵. Since this method works per sample, we applied it on correctly predicted samples in the test sets. We included samples with only one label for further interpretability. Finally, we averaged feature attributions across selected samples, and scaled them by dividing to the maximum attribution.

Proteome-wide inference

MOI and molecular mechanism inference After selecting the final models for MOI and functional effect prediction, we predicted the MOI for all proteins in the PPI network (Supplementary Table 5). Afterwards, we predicted the functional effect for the subset of proteins that were predicted as AD or ADAR (Supplementary Table 6).

Enrichment analysis To study further the predictions, we used GSEAPy⁵⁶ to perform enrichment analysis⁵⁷, which is a statistical method used to determine whether known biological functions or processes are over-represented in a protein list of interest (e.g. AD proteins). In this method, the enrichment significance is calculated based on the hypergeometric distribution, where p-value is the cumulative probability of observing at least k proteins of interest annotated to a specific protein set. The formula for the p-value is given by:

$$p = 1 - \sum_{i=0}^{k-1} \frac{\binom{M}{i} \binom{N-M}{n-i}}{\binom{N}{n}},$$

where N is the total number of proteins in the background distribution, M is the number of proteins in that distribution annotated to the gene set of interest, n is the size of the list of proteins of interest, and k is the number of proteins in that list which are annotated to the gene set. We focused on pathways containing at least 10 and at most 500 genes to exclude pathways that are either too specific or too general. As a reference database, we used Gene Ontology (Biological Processes)^{58,59} to understand functional landscape of proteins.